ARTICLE
Journal of Cellular Biochemistry 116:1602–1612 (2015)

Journal of Cellular Biochemistry

Timely Degradation of Wip1 Phosphatase by APC/C Activator Protein Cdh1 is Necessary for Normal Mitotic Progression

Ho-Chang Jeong,[1] Na-Yeon Gil,[1] Ho-Soo Lee,[2,3] Seung-Ju Cho,[1] Kyungtae Kim,[4] Kwang-Hoon Chun,[5] Hyeseong Cho,[2,3] and Hyuk-Jin Cha[1]*

[1]*College of Natural Sciences, Department of Life Sciences, Sogang University, Seoul, Korea*
[2]*Department of Biochemistry, Ajou University School of Medicine, Suwon, Korea*
[3]*Genomic Instability Research Center, Ajou University School of Medicine, Suwon, Korea*
[4]*National Cancer Center, Goyang-si, Gyeonggi-do, Korea*
[5]*Gachon Institute of Pharmaceutical Sciences, College of Pharmacy, Gachon University, Incheon, Korea*

ABSTRACT

Wip1 belongs to the protein phosphatase C (PP2C) family, of which expression is up-regulated by a number of external stresses, and serves as a stress modulator in normal physiological conditions. When overexpressed, premature dephosphorylation of stress-mediators by Wip1 results in abrogation of tumor surveillance, thus Wip1 acts as an oncogene. Previously, the functional regulation of Wip1 in cell-cycle progression by counteracting cellular G1 and G2/M checkpoint activity in response to DNA damage was reported. However, other than in stress conditions, the function and regulatory mechanism of Wip1 has not been fully determined. Herein, we demonstrated that protein regulation of Wip1 occurs in a cell cycle-dependent manner, which is directly governed by APC/C^{Cdh1} at the end of mitosis. In particular, we also showed evidence that Wip1 phosphatase activity is closely associated with its own protein stability, suggesting that reduced phosphatase activity of Wip1 during mitosis could trigger its degradation. Furthermore, to verify the physiological role of its phosphatase activity during mitosis, we established doxycycline-inducible cell models, including a Wip1 wild type (WT) and phosphatase dead mutant (Wip1 DA). When ectopically expressing Wip1 WT, we observed a delay in the transition from metaphase to anaphase. In conclusion, these studies show that mitotic degradation of Wip1 by APC/C^{Cdh1} is important for normal mitotic progression. J. Cell. Biochem. 116: 1602–1612, 2015.

KEY WORDS: Wip1; MITOSIS; APC/C^{Cdh1}; MITOTIC PROGRESSION; ANAPHASE TRANSITION; ATM

The wild-type, p53-induced phosphatase 1 (Wip1, encoded by PPM1D) was initially identified as a member of the protein phosphatase 2C (PP2C) family of serine/threonine phosphatases, which has Mg^{2+}-dependent phosphatase activity and is insensitive to okadaic acid [Fiscella et al., 1997]. Wip1 is induced in response to DNA damage stimuli such as ionization radiation (IR), reactive oxygen species (ROS) and other genotoxic agents in a p53-dependent manner [Xia et al., 2009; Douarre et al., 2013]. Consequently, it is regarded as a homeostatic modulator of a number of stress pathways because Wip1 preferably dephosphorylates pivotal stress-mediators with conserved phosphorylation moieties, i.e., p(S/T)Q or pTXpY site, including H2AX (139pS), p53 (15pS), ATM (1981pS), Chk1 (345pS), Chk2 (68pT) and p38 (180pT) [Yamaguchi et al., 2007; Cha et al., 2010; Ciccia and Elledge, 2010; Lowe et al., 2012]. Thereby, when Wip1 is overexpressed, which is frequently observed in many types of cancers, oncogenic progression can readily occur due to premature abrogation of the tumor surveillance network [Lowe et al., 2012]. In addition, other than in cancer or stress signaling, the functional role of Wip1 has not been extensively explored. For example, Wip1 plays roles in autophagy to control obesity and atherosclerosis [Le Guezennec et al., 2012], in neutrophil migration and inflammation [Sun et al., 2014], and even in heterochromatin silencing [Filipponi et al., 2013].

Conflict of interest: None
Grant sponsor: National Research Foundation of Korea (NRF); Grant sponsor: Korean Government (MSIP); Grant numbers: 2011-0030043, 2009-0093822, 2013075411.
*Correspondence to: Hyuk-Jin Cha, Ph.D., Department of Life Sciences, Sogang University, Seoul 121-742, Korea. E-mail: hjcha@sogang.ac.kr
Manuscript Received: 22 July 2014; Manuscript Accepted: 23 January 2015
Accepted manuscript online in Wiley Online Library (wileyonlinelibrary.com): 3 February 2015
DOI 10.1002/jcb.25114 • © 2015 Wiley Periodicals, Inc.

Of interest, p(S/T)Q motifs in Wip1 substrates such as H2AX, p53, Chk1 and Chk2 are mostly phosphorylated by PI3K-like kinases such as ATM, which suggests that Wip1 may serve as a major phosphatase to dampen the ATM-mediated stress response (e.g., cell cycle arrest at G1 or G2) upon DNA damage [Yamaguchi et al., 2007]. A recent study revealed that Wip1 contributes to recovery from G2 arrest by modulating the p53-mediated gene response upon DNA damage [Shaltiel et al., 2014].

Given that Wip1 controls ATM activity or ATM-dependent substrate phosphorylation, a novel function of Wip1 is identified when novel functions of ATM are disclosed [Le Guezennec et al., 2012; Filipponi et al., 2013]. Although ATM-dependent G1 or G2 arrest after DNA damage has been well-characterized, the roles of ATM during normal mitosis through ATM-dependent phosphorylation of mitotic proteins [Matsuoka et al., 2007] have only been limitedly examined [Oricchio et al., 2006; Shen et al., 2006]. In a previous study, ATM was demonstrated to be important in the spindle assembly checkpoint through phosphorylating Budding uninhibited by benzimidazoles 1 (Bub1) [Yang et al., 2011], which suggests that the phosphorylation status of mitotic substrates of ATM is also important in controlling normal mitotic progression. Recently, Macurek et al. [2013] demonstrated that a Wip1 protein with decreased phosphatase activity is downregulated during mitosis and that ectopic expression of Wip1 failed to influence normal mitotic progression.

In this study, we also found that the expression levels of Wip1 phosphatase were decreased during mitosis and that its regulation was mediated by APC/C^{Cdh1}-dependent protein degradation rather than a change in transcriptional levels, as shown in a previous study [Macurek et al., 2013]. Furthermore, by taking advantage of the Wip1 inducible H2B-GFP-HeLa cell line, we found that timely induction of Wip1 wild type (WT), but not a phosphatase-dead (DA) mutant, during mitosis significantly delayed normal mitotic progression, suggesting that timely reduction of its phosphatase activity or protein level may be important for normal mitotic exit. Our results provide a novel perspective in which the phosphorylation status of certain mitotic targets of Wip1 would be necessary for normal mitotic progression.

MATERIALS AND METHODS

CELL CULTURE

MCF7 and H2B-GFP-HeLa cells (expressing green fluorescent protein (GFP)-fused Histone H2B protein), were maintained in DMEM supplemented with 10% fetal bovine serum (FBS) and 50 μg/ml gentamycin (Gibco, 15750-060) at 37°C in a humidified 5% CO_2 incubator. H1299 cells were maintained in RPMI Medium 1640 supplemented with 10% fetal bovine serum and 50 μg/ml gentamycin.

GENERATION OF Wip1 INDUCIBLE CELL LINES

CSIV-TRE-RfA-UbC-KT lentiviral plasmids expressing doxycycline-inducible Wip1 WT or DA were constructed using Gateway Technology with Clonase II (Invitrogen) as described previously [Kurita et al., 2013]. The following primers were used: attB-Wip1-S: 5′-GGGGACAAGTTTGTACAAAAAAGCAGGCTTCACCATGGCGGGGCTGTACTCGCTG-3′, attB-Wip1-AS: 5′-GGGGACCACTTTGTACAAGAAAGCTGGGTCTCAGCAAACACAAACAGTTTT-3′. The lentiviruses containing doxycycline-inducible Wip1 WT or DA were produced using ViraPower Lentiviral expression system in 293FT cells (Invitrogen). Briefly, 293FT cells were transfected with this lentiviral plasmid and three packaging plasmids (pLP1, pLP2, and pLP/VSVG) at a ratio of 1:3. The supernatants were collected at 48 h post-transfection, filtered, and then transduced into HeLa-H2B-GFP cells at a 1:1 ratio twice. The GFP/Kusabira-Orange double positive cells were sorted by FACS.

REAGENTS AND ANTIBODIES

Nocodazole (Cat# M1404) and CCT007093 (Cat# C9369) were purchased from Sigma–Aldrich. Thymidine (Cat# 194754) was obtained from MP biomedical. MG132 (Cat# 474790) was bought from Calbiochem. Cyclohexamide (Cat# 54646) was acquired from Biomol. The anti-protein phosphatase 1D (PPM1D) antibody (A300-664A) was acquired from Bethyl Laboratories. The antibodies against ERK2 (Sc-154), proliferating cell nuclear antigen (PCNA) (Sc-56), Cyclin B1 (Sc-245), Securin (Sc-56207), HA (Sc-7392), Myc (Sc-40), β-actin (Sc-47778), and α-tubulin (Sc-8035) were obtained from Santa Cruz Biotechnology, Inc. The anti-Histone H3 (phospho-Ser10) antibodies for western blotting (LF-PA20214) and for flow cytometry (ab14955) was bought from Abfrontier and Abcam, respectively. The antibodies against pCDK2 (T160, #2561), cleaved poly (ADP-ribose) polymerase (PARP) (#5625), phospho-H2AX (S139, #9718), cleaved caspase 9 (#9505), and α/β tubulin (#2148) were purchased from Cell signaling Technology.

CELL SYNCHRONIZATION

Cells were synchronized at the G1/S boundary using double thymidine block (DTB). In brief, cells were initially treated with 2.5 mM thymidine for 16 h. After removal of the thymidine, the cells were incubated in fresh medium for 8 h, and then 2.5 mM thymidine as a final concentration was added for an additional 16 h. Following removal of the thymidine, the cells were incubated in fresh medium, and then harvested at respective time points. In order to perform the thymidine-nocodazole block, cells were initially synchronized at the G1/S boundary with 2.5 mM thymidine for 24 h, and then incubated in fresh medium including nocodazole (50 ng/ml) for 12 h. After mitotic shake-off, the cells were released into fresh medium at different time points.

WESTERN BLOTTING

Cells were rinsed in phosphate-buffered saline (PBS) twice, and then lysed with tissue lysis buffer (TLB) (20 mM Tris–HCl, pH 7.4, 137 mM NaCl, 2 mM EDTA, 1% Triton X-100, and 10% glycerol) supplemented with 0.2 mM sodium vanadate and 1 mM protease inhibitor cocktail (Roche, 11873580001) on ice for 30 min to extract soluble and membrane-bound proteins. Approximately 10–20μg of total proteins were separated on a 10% or 12% sodium dodecyl sulphate-polyacrylamide gel electrophoresis (SDS-PAGE). The proteins were transferred to polyvinylidene fluoride (PVDF)-membrane, and then blocked for 1–2 h in Tris-buffered saline with 0.1% Tween-20 (TBS-T) with 5% non-fat dry milk. The membrane was incubated with specific

primary antibodies (1:1000) in TBS-T at 4°C overnight, and then washed in TBS-T for each 5 min three times, followed by incubation with HRP-conjugated secondary antibodies (1:10000) (Jackson Immunoresearch Laboratories) at room temperature for 1 h. Finally, immunoreactivity was measured by enhanced chemiluminescence detection system (Amersham Biosciences).

IMMUNOPRECIPITATION AND IN VIVO UBIQUITYLATION ASSAY

Cells were rinsed with PBS twice, lysed in TLB, and centrifuged at 13,000 rpm at 4°C for 10 min. Approximately 100–500 μg of total proteins were incubated with 1 μg of specific primary antibodies at 4°C overnight, followed by addition of Protein G Sepharose (GE health, 17-0618-01) or Protein A Sepharose (GE health, 17-0780-1) beads, and then incubated at 4°C for an additional 4 h. The precipitates were washed with TLB for each 20 min three times, and then separated by SDS-PAGE. Western blotting was conducted using standard methods. For in vivo ubiquitylation assay, synchronized cells by the thymidine-nocodazole block were treated with 5 μM MG132 for 12 h before harvesting.

IMMUNOFLUORESCENCE

Cells were fixed with 4% paraformaldehyde for 10–15 min, and then permeabilized with 0.1% Triton X-100 in PBS for 5 min. The fixed cells were incubated for 1–2 h in TBS-T containing 3% bovine serum albumin (BSA) for blocking, followed by incubation with the PPM1D antibody (1:200) in TBS-T containing 3% BSA at 4°C overnight. The cells were washed in TBS-T for each 5 min three times, and then incubated with the Alexa 594-conjugated secondary antibody (1:200) and 0.5 μg/ml 4′,6-diamidino-2-phenylindole (DAPI) for cellular DNA staining.

PLASMID DNA, siRNA OLIGONUCLEOTIDE AND RECOMBINANT WIP1

HA-tagged ubiquitin, Myc-tagged Cell division cycle 20 (Cdc20) and HA-tagged Cdh1 expression vectors were previously described [Cho et al., 2012]. The day before transfection, cells were seeded at approximately 5×10^6 in 10-cm plates. In brief, 6 μg of each plasmid was transfected into cells using Lipofectamine 2000 (Invitrogen, 11668-027) in accordance with the manufacturer's instruction. The human Cdh1 siRNA (5′-AATGAGAAGTCTCCCAGTCAG-3′) was previously described [Cotto-Rios et al., 2011]. The siRNA was transfected into H2B-GFP-HeLa expressing inducible Wip1WT cells in the presence of 0.1 μg/ml doxycycline using Dharma-FECT (Thermo Scientific) according to the manufacturer's instructions. The recombinant human Wip1 proteins were previously isolated from bacteria [Belova et al., 2005].

QUANTITATIVE REAL-TIME PCR

Total RNA was extracted from cells using Total RNA Extraction Kit (Intron, 17061), and then converted to cDNA using PrimeScript RT Master Mix (Takara, RR036) in accordance with the manufacturer's instruction. The synthesized cDNAs were used as templates to perform the real-time PCR with LightCycler 480 Instrument II (Roche) using SYBR Premix Ex Taq (Takara, RR420) under the following conditions: denaturation at 95°C for 30 s, followed by 40 cycles of 95°C for 5 s, 58°C for 15 s, and 72°C for 20 s. For validation of PCR, the amplified products were separated on 2% agarose gel and then visualized via ethidium bromide staining. Used gene-specific primers were as follows: Wip1 (5′-TACCTGAACCTGACTGACAG-3′, 5′-CGAGCTATCTCAGCTGAAAC-3′), β-actin (5′-GTCCTCTCCCAAGTCCACAC-3′, 5′-GGGAGACCAAAAGCCTTCAT-3′, GAPDH (5′-GTGATGGCATGGACTGTGGT-3′, 5′-AAGGGTCATCATCTCTGCCC-3′).

FLOW CYTOMETRY

Cells were initially synchronized with double thymidine block, and then collected at respective time points after the release from this block. The cells were washed in PBS twice, and then fixed with chilled 70% ethanol at 4°C overnight. The fixed cells were rinsed in PBS twice, and then incubated with RNaseA (60 μg/ml, Invitrogen, 12091-021) and propidium iodide (40 μg/ml, Sigma, P4170) at 37°C for 30 min in dark room, followed by analyzed on a BD FACSCalibur (BD Biosciences). For measuring the pHH3-positive cells, cells were fixed in ice-cold 80% methanol drop by drop at 4°C overnight. The fixed cells were permeabilized 0.25% Triton X-100 in PBS for 5 min on ice, and then incubated with 5 μg/ml anti-Histone H3 (phospho S10) antibody in PBS containing 1% BSA at 4°C overnight with gentle agitation. Following washing with PBS, the cells were incubated with 1.2 μg/ml anti-mouse Peridinin chlorophyll protein (PerCP)-conjugated secondary antibody (F0114) in PBS containing 1% BSA at room temperature for 1 h, washed with PBS, and analyzed by the flow cytometer.

LIVE-CELL IMAGING

H2B-GFP-HeLa cells were synchronized at the G1/S boundary by double thymidine block. The arrested cells were incubated on the microscope in CO_2-independent medium (Invitrogen) supplemented with 10% FBS, 100 U/ml penicillin G, and 0.1 mg/ml streptomycin at 37°C in a 5% CO_2 chamber. Time-laps images were acquired using a Nikon eclipse Ti with a 20 × 1.4 NA Plan-Apochromat objective every 5 min for 24 h. Images were captured with an iXonEM +897 Electron Multiplying CCD camera and controlled using NIS elements Ar microscope imaging software.

STATISTICAL ANALYSIS

Graphical data are presented as mean ± SD. Statistical significance among three groups and between groups were determined using one-way or two-way analysis of variance (ANOVA) following Bonferroni multiple comparison post-test and Student's *t*-test, respectively.

RESULTS

CELL CYCLE-SPECIFIC Wip1 REGULATION

To determine Wip1 protein levels during the cell cycle, the MCF7 cell line, which is a breast cancer cell line highly expressing Wip1 [Bulavin et al., 2002], was synchronized at the G1/S boundary by a double thymidine block (DTB) and then released back into normal cell cycle. At 13 h after release from this block, the levels of phospho-Histone H3 (pHH3, S10) increased, indicating mitosis. In contrast, the levels of Wip1 protein significantly decreased at 13 h post-thymidine release (Fig. 1A). For more precise cell cycle synchrony, HeLa S3 cells,

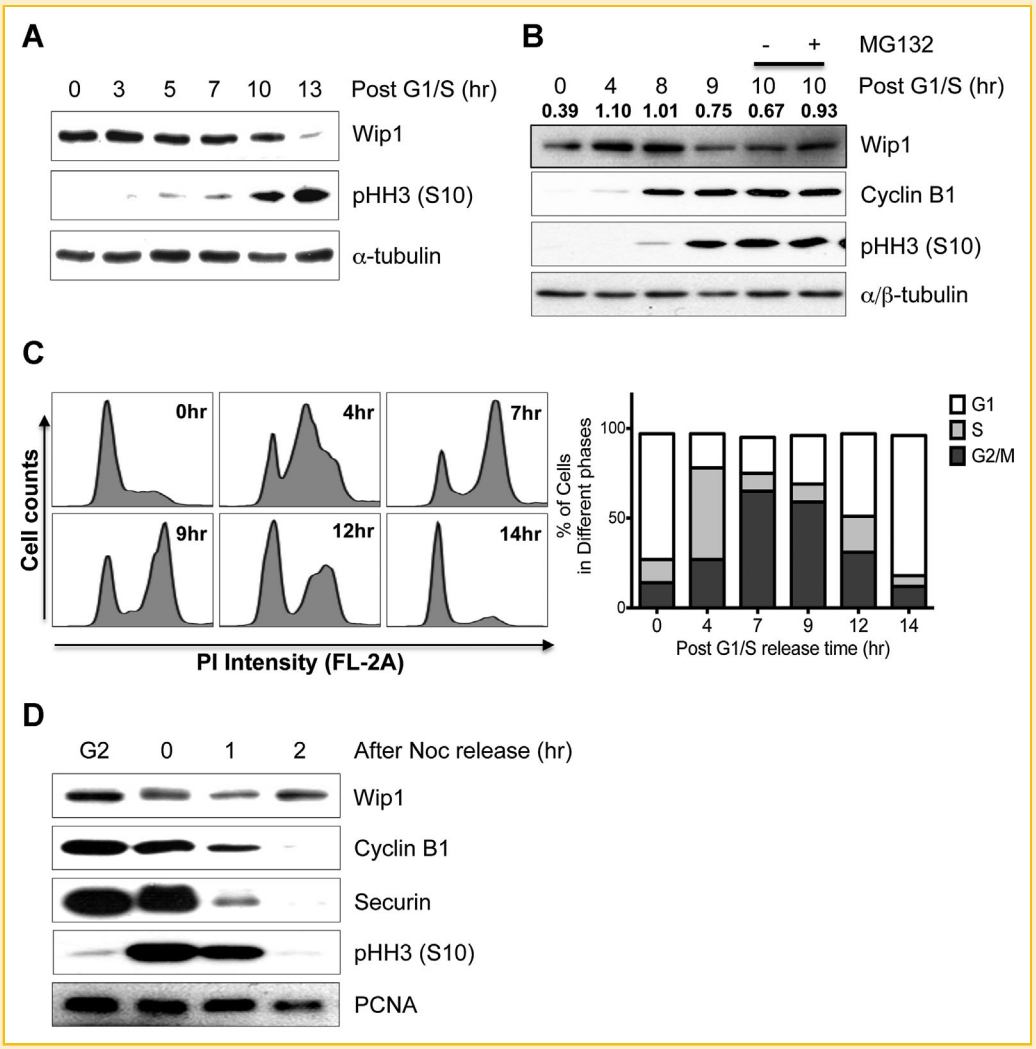

Fig. 1. Wip1 decreases at mitosis during the cell cycle. (A) MCF7 and (B) HeLa S3 cells were synchronized at the G1/S boundary and then released until the indicated time points. Western blotting was performed using the indicated antibodies, and 10 μM MG132 was incubated for 1 h before harvesting. The band intensity of Wip1 was normalized against α/β tubulin and then presented. (C) The cell cycle synchrony of HeLa S3 cells was analyzed by flow cytometry with propidium iodide. The percentage of cells in the different phases at each respective time was represented by a stacked bar graph (right panel). (D) MCF7 cells were synchronized by a thymidine–nocodazole block. Samples were collected at the indicated times after mitotic shake-off and subjected to immunoblotting analysis. PCNA served as a protein-loading control.

which widely used in normal cell cycle study, were utilized. Consistently, the levels of Wip1 protein were maintained for several hours after G1/S release and began to disappear at mitosis, as evidenced by the dramatic increase in the pHH3 levels at 9–12 h. Of note, Wip1 protein level, which was significantly decreased at 10 h, was slightly recovered by just 1 h pretreatment of MG132, a proteasome inhibitor (Fig. 1B). To confirm that the cell cycle was synchronized correctly under this experimental condition, each stage of the cell cycle of HeLa S3 cells was further determined by flow cytometric analysis after G1/S release. As shown in Figure 1C, timely progression of the cell cycle was observed at 4 h (S phase), 7 h (G2 phase), 9 h (mitosis), 12 h (end of mitosis) and 14 h (G1 phase) post-thymidine release, supporting that Wip1 was downregulated during mitosis in a timely manner. We further investigated which sub-phases during mitosis were considerably responsible for Wip1 down-regulation. To answer this question, MCF7 cells were synchronized at prometaphase by a thymidine-nocodazole block, and most mitotic cells were collected by mitotic shake-off, while G2 cells were simply acquired from the remaining adherent cells [Cho et al., 2012]. Interestingly, the levels of Wip1 protein in mitosis appeared to be markedly reduced until 1 h post-nocodazole release and then increased in G1 phase. Both significantly reduced levels of Securin and Cyclin B1 with constant levels of phospho-Histone H3 (pHH3, S10) showed that a time course of 1 h post-nocodazole release represented the anaphase during mitosis (Fig. 1D). Therefore, these data indicate that Wip1 expression levels begin to be specifically reduced at mitosis during the cell cycle, in particular, metaphase-to-anaphase transition.

UBIQUITIN DEPENDENT DOWN REGULATION OF Wip1 DURING MITOSIS

To test the possibility that Wip1 mitotic downregulation results from the suppression of Wip1 mRNA expression, we determined the mRNA levels during the cell cycle by real-time PCR analysis. However, there was no remarkable change in the Wip1 mRNA levels during the cell cycle in HeLa S3 cells (Fig. 2A).

As mitotic protein downregulation is mostly governed by ubiquitin-mediated proteolysis during cell cycle control [Nakayama and Nakayama, 2006; Teixeira and Reed, 2013], it is readily surmised that Wip1 would also undergo ubiquitin-mediated proteolysis during mitosis. To prove this hypothesis, we utilized MG132, to rescue the protein from ubiquitin-mediated proteolysis. Because mitotic progression can also be affected by MG132 treatment, which would block proper, timely proteolysis of mitosis-specific proteins within cells, an in vitro cell-free system was adopted to measure the effect of MG132 on Wip1 protein degradation and exclude undesirable bias. As shown in Figure 2B, the Wip1 recombinant protein was markedly reduced when it was incubated with mitotic cell lysate compared to that from G1/S phase, with clear phosphorylation of nucleophosmin (NPM), which only occurs during mitosis [Cha et al., 2004; Zhang et al., 2004]. In contrast, the degradation of Wip1 was markedly reduced by MG132 treatment in the mitotic cell lysate as well as in vivo cell system (Fig. 1B), indicating that Wip1 underwent proteasome-dependent degradation during mitosis. To further examine whether Wip1 is subject to ubiquitination, Wip1 expression was induced in a doxycycline (Dox)-inducible cell line (H1299 cells) [Cha et al., 2010] after HA-ubiquitin was introduced, and ubiquitination of Wip1 was

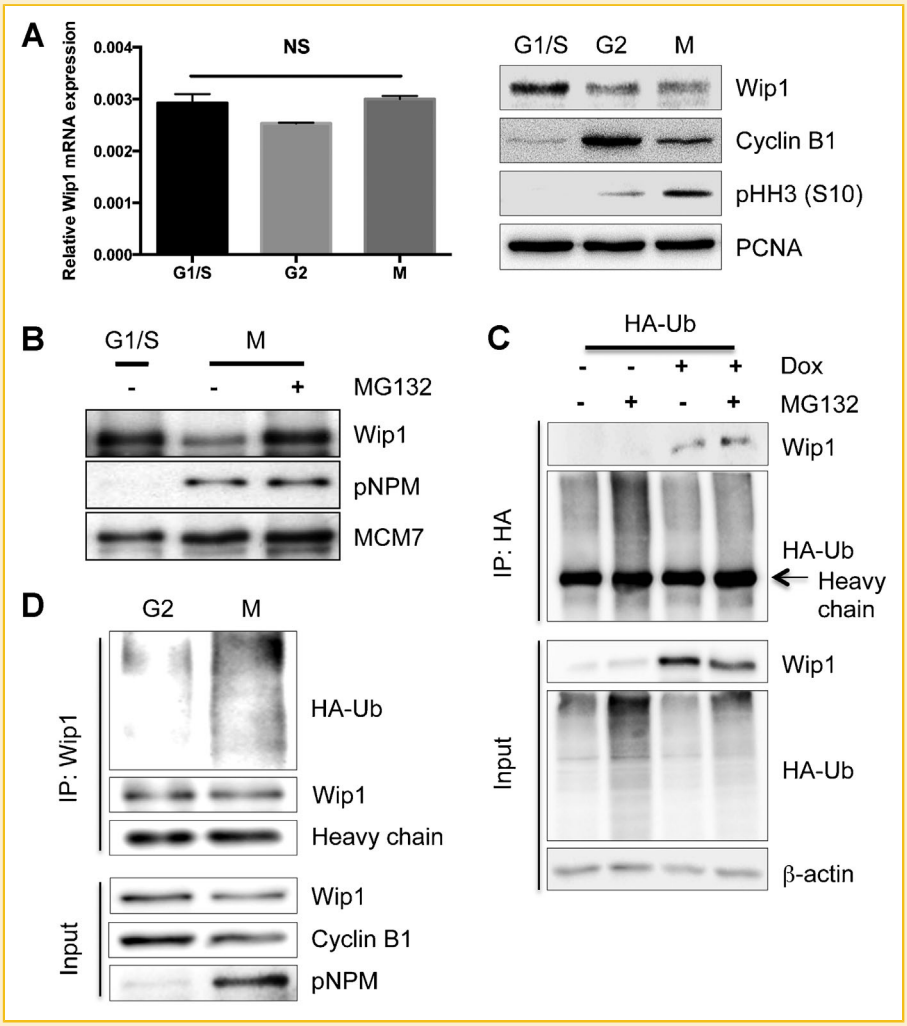

Fig. 2. Wip1 is down-regulated by the ubiquitin-proteasome pathway. (A) HeLa S3 cells were synchronized by a DTB, released with fresh media, and then harvested at G1/S phase (0 h), G2 phase (7 h), and mitosis (10 h). The extracted RNAs were quantified by real-time PCR analysis. β-actin for loading control. Immunoblot data show each phase of cell cycle. (B) Recombinant Wip1 proteins were incubated with G1/S or mitotic lysates from 293T cells in the absence or presence of 10 μM MG132 for 2 h in vitro. pNPM was used as a mitotic marker. MCM7 was used for equal protein loading. (C) Ectopically expressed HA-ubiquitin in H1299 cells was immunoprecipitated (IPed) with HA antibody. The Wip1 protein (induced by 0.5 μg/ml Dox) level in HA-ubiquitin immunoprecipitates after induction in the absence or presence of 5 μM MG132 was determined by subsequent immunoblotting analysis. (D) Wip1 was IPed from G2 or mitotic cells of inducible iWip1-H2B-GFP-HeLa Wip1 cells after HA-ubiquitin expression and subjected to immunoblotting for HA-ubiquitin.

monitored by immunoprecipitation (IP) using the anti-HA antibody followed by immunoblotting (IB) with Wip1 antibody. Wip1 binding to ubiquitin was clearly observed when Wip1 was induced (Fig. 2C). As it is plausible to investigate the ubiquitination of Wip1 protein relative to mitosis, we further utilized H2B-GFP-HeLa cells to monitor mitotic phase. We introduced the CSIV-TRE-RfA-UbC-KT vector [Kurita et al., 2013] containing the Wip1 wild type (WT) or Wip1 phosphatase dead mutant (DA) [Cha et al., 2010] into H2B-GFP-HeLa cells to generate Wip1-inducible HeLa cell lines. Due to the presence of humanized Kusabira-Orange 1 (hKO1) fluorescent protein, H2B-GFP-HeLa cells transfected with the CSIV-TRE-RfA-UbC-KT vector were detected well using red fluorescence (Red, Fig. S1A). Cells expressing inducible Wip1 WT or DA vectors were further treated with various concentrations of Dox to determine a concentration for the equivalent Wip1 expression between WT and DA (WT: 0.05 μg/ml and DA: 0.5μg/ml of Dox) (Fig. S1B). Upon Dox treatment, Wip1 expression appeared to be retained for 16 h and then decreased thereafter (Fig. S1C). By taking advantage of the newly established, Wip1-inducible H2B-GFP-HeLa cells (iWip1-H2B-GFP-HeLa), we examined the mitosis-specific ubiquitination of Wip1. HA-ubiquitin was first introduced into iWip1-H2B-GFP-HeLa cells, and the cells were then subjected to DTB followed by nocodazole with Dox treatment to collect only the mitotic population using mitotic shake-off. The undetached population during mitotic shake-off can be considered the G2 population [Cho et al., 2012]. Wip1 induced by Dox treatment at G1/S was equivalently expressed in the G2 and mitotic populations (Fig. 2D, the first panel). Extracted Wip1 was then subjected to IB for HA to determine the associated ubiquitination level. As predicted, multiple ubiquitination signals were significantly increased in Wip1 extracted from the mitotic population than that of the G2 population (Fig. 2D).

INVOLVEMENT OF APC/C^{CDH1} IN WIP1 DOWN-REGULATION

Cell cycle-regulatory E3 ligases play an important role in degradation of the cell-cycle machinery [Peters, 1998]. In particular, APC/C$^{Cdc20\ or\ Cdh1}$ specifically govern mitotic regulatory proteins as well as Cyclins, of which timely degradation is essential for the onset of the metaphase-anaphase transition [Peters, 2002; Peters, 2006; Manchado et al., 2010]. To examine the involvement of either Cdc20 or Cdh1 in endogenous Wip1 mitotic degradation, MCF7 cells were transfected with Cdc20 (C20) or Cdh1 (C1) in the absence or presence of MG132. Immunoblot analysis showed that the Wip1 protein levels were also decreased by Cdh1 (Fig. 3A). Furthermore, the suppressed Wip1 protein levels were recovered by incubation with MG132, indicating that Wip1 expression was regulated by a Cdh1-dependent proteasomal degradation pathway. As Cdc20- as well as Cdh1-dependent APC activity is supposedly fully activated during mitosis, endogenous Wip1 downregulation by Cdh1 would also occur during mitosis. For this reason, the Wip1 protein levels were monitored in mitotic MCF7 cells collected by shake-off after transfection of either Cdc20 or Cdh1. Consistent with the result in Figure 3A, the Wip1 protein levels under Cdh1 expression were also reduced as similar as that of Cdc20, while MG132 treatment rescued Wip1 downregulation (Fig. 3B). Therefore, Wip1 ubiquitination upon ectopic expression of ubiquitin should be increased in the presence of Cdh1 activity during mitosis. When Cdh1 and ubiquitin were co-transfected into iWip1-H2B-GFP-HeLa cells in the presence of Dox, the ubiquitination of ectopic Wip1 was clearly increased without affecting the cell cycle, while the level of phosphorylated BubR1, which occurs during mitosis due to the action of Plk1 [Elowe et al., 2007], remained unaltered regardless of Cdh1 or ubiquitin expression (Fig. 3C). Level of ubiquitination toward Wip1 between Cdc20 and Cdh1 appeared to be comparable when Cdc20 or Cdh1 was co-transfected with ubiquitin (Fig. S2). When Cdh1-siRNA-transfected iWip1-H2B-GFP-HeLa cells in the presence of Dox were released from G2/M, the Wip1 protein levels were markedly increased and sustained throughout mitosis when compared to the control. Cyclin B1, a known-target of Cdh1-mediated APC action [Raff et al., 2002], was used as a positive control (Fig. 3D). To evaluate if Wip1 can be a direct target of the APC/C^{Cdh1} ubiquitin ligase, we next attempted to find the recognition motifs of APC/C^{Cdh1}, such as a destruction box (D-box) or a KEN-box, using the GPS-ARM software (http://arm.biocuckoo.org/faq.php) [Liu et al., 2012]. From the results, we were able to predict that human Wip1 has a D-box with a consensus sequence of RxxL (where X is any amino acid) at amino acids 76–79 (data not shown). Based on the prediction, mitotic Wip1 downregulation may be governed by direct interaction between APC/C^{Cdh1} and Wip1. Thereby, the protein interaction between Cdh1 and Wip1 was examined. As shown in Figure 3E and 3F, Wip1 was found to directly interact with Cdh1. These data indicate that APC/C^{Cdh1} is responsible for Wip1 ubiquitination and degradation during mitosis.

THE EFFECT OF THE PHOSPHATASE ACTIVITY OF WIP1 ON ITS STABILITY

Wip1 protein downregulation during diverse events other than the cell-cycle process was reported in multiple studies [Zhang et al., 2010; Crescenzi et al., 2013]. We also observed that the Wip1 protein levels were markedly downregulated after ultra-violet (UV) exposure [Lee et al., 2014]. Of note, we also observed that Wip1 chemical inhibitor treatment facilitated Wip1 protein downregulation [Lee et al., 2014], suggesting that Wip1 protein downregulation might be controlled by its own phosphatase activity. Supporting this idea, Wip1 phosphatase activity during mitosis, when Wip1 is subject to protein degradation, was weakened by increased phosphorylation of Wip1 by active CDK1 [Macurek et al., 2013]. Therefore, we surmised that loss of Wip1 phosphatase activity would be linked to a signal for Wip1 degradation. To validate the previous observation, MCF7 cells were treated with CCT007093 (CCT), a commercially available chemical inhibitor of Wip1 [Rayter et al., 2008]. Interestingly, the levels of Wip1 protein were significantly reduced by treatment with CCT compared to the control, and the Wip1 protein level remained unaltered by CCT treatment in the presence of MG132 (Fig. 4A). In the same condition, Wip1 mRNA levels remained constant, showing that Wip1 phosphatase activity can affect its own integrity at the post-translational level (Fig. 4B). Thus, these results suggest that inhibition of Wip1 phosphatase activity could trigger the molecular machinery to promote Wip1 destruction. To avoid off-target effects of CCT on JNK activity, which could introduce unexpected bias in Wip1 downregulation, as shown previously in cells with low expression of Wip1 [Lee et al., 2014], we next took advantage of the Wip1 WT- and DA-inducible system. The half-lives of equivalently induced Wip1 WT and DA by Dox treatment were determined after treatment with

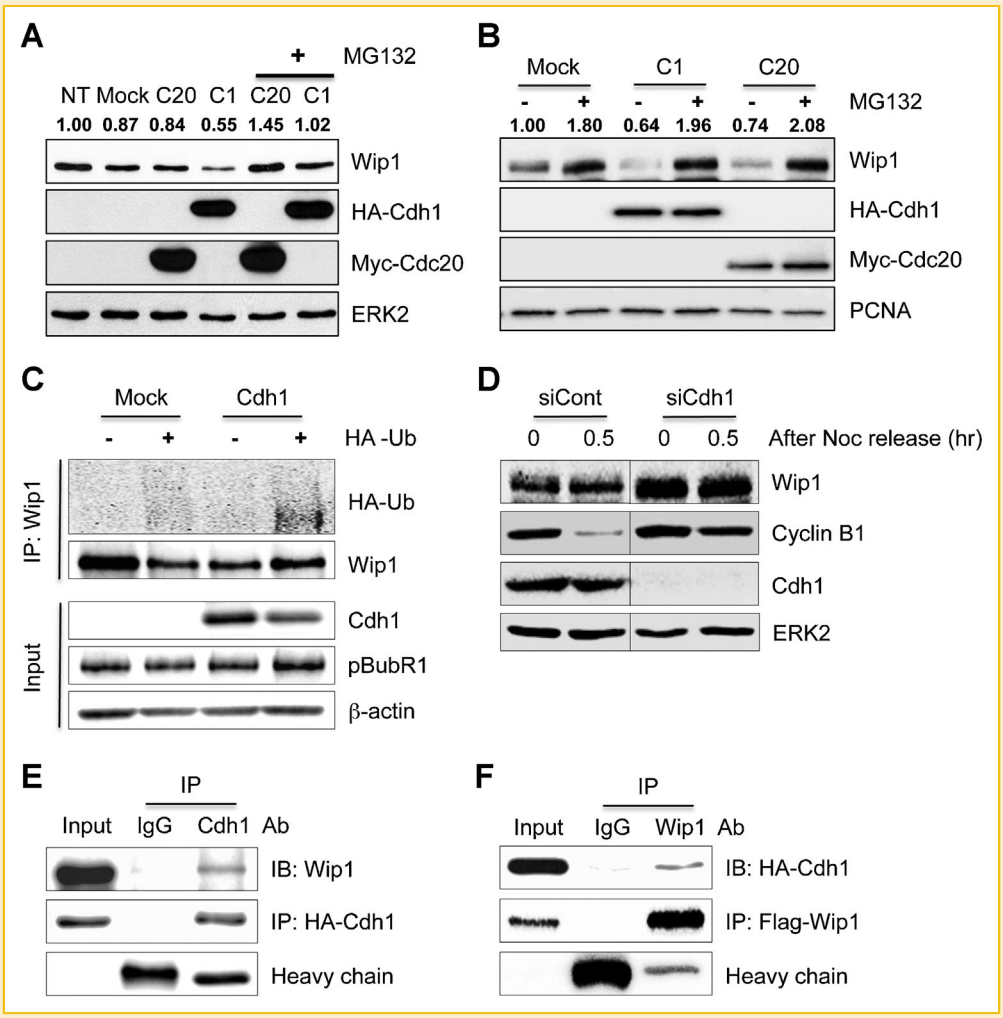

Fig. 3. APC/C^{Cdh1}-dependent Wip1 down-regulation. The Wip1 protein levels in asynchronous MCF7 cells (A) and mitotic lysates (B) expressing either Myc-Cdc20 or HA-Cdh1 were determined by immunoblotting analysis. MG132 (10 μM) was added for 6 h. ERK2 (A) or PCNA (B) served as protein-loading controls. The band density of Wip1 was quantified versus ERK2 (A) and PCNA (B), respectively. (C) HA-Cdh1 and/or HA-ubiquitin were expressed in iWip1-H2B-GFP-HeLa cells. The ubiquitin level of Wip1 was determined by IP for Wip1 followed by IB for HA-ubiquitin. β-actin served as a protein-loading control. (D) The mitotic Wip1 protein levels after mitosis release (0.5 h) were determined in iWip1-H2B-GFP-HeLa cells transfected with mock (siCont) or Cdh1 siRNA (siCdh1) in the presence of Dox (0.1 μg/ml). ERK2 served as a protein-loading control. (E) iWip1-H2B-GFP-HeLa cells were transfected with HA-Cdh1 in the presence of Dox (0.5 μg/ml). HA-Cdh1 was IPed, and Wip1 binding was determined by IB with a Wip1 antibody. (F) 293T cells were co-transfected with HA-Cdh1 and Flag-Wip1. Flag-Wip1 was IPed, and reciprocal interaction of Cdh1 was confirmed by IB with a HA antibody.

CHX. As shown in Figure 4C, the DA mutant, which showed no apparent phosphatase activity toward p38 [Bulavin et al., 2004], as well as H2AX [Cha et al., 2010] (Fig. S1D) were more promptly degraded compared to WT (Fig. 4C). The half-life of DA mutant was close to 4 h, whereas that of Wip1 was close to 8 h (Fig. 4C). Taken together, these data demonstrate that downregulation of Wip1 during mitosis correlates with the loss of its phosphatase activity.

ESSENTIAL ROLE OF WIP1 DOWN-REGULATION AT THE METAPHASE-ANAPHASE TRANSITION

Considering the fact that a number of mitotic regulatory proteins, such as Plk1 and Cyclin B1, are supposed to be degraded by APC/C during mitosis, we surmised that timely Wip1 mitotic downregulation would also be important for proper mitotic progression once their timely mitotic action became dispensable. Given that ATM is activated during mitosis and serves as an important mitotic regulator [Yang et al., 2011], ATM-dependent phosphorylation (pS/TQ motif), which targets a common site with Wip1 [Yamaguchi et al., 2007], may remain sustained when Wip1 undergoes protein degradation. Thus, timely induction of Wip1 WT, but not DA, during mitosis, which may alter various protein phosphorylation statuses, could affect mitotic progression. Such an assumption could be well supported by recent data showing that mitotic Wip1 phosphatase activity is significantly weakened by Cyclin-dependent kinase 1 (Cdk1)-dependent phosphorylation [Macurek et al., 2013].

To prove the effect of prolonged phosphatase action of Wip1 toward mitotic progression, iWip1-H2B-GFP-HeLa cells were synchronized at G1/S and released back to the normal cycle with

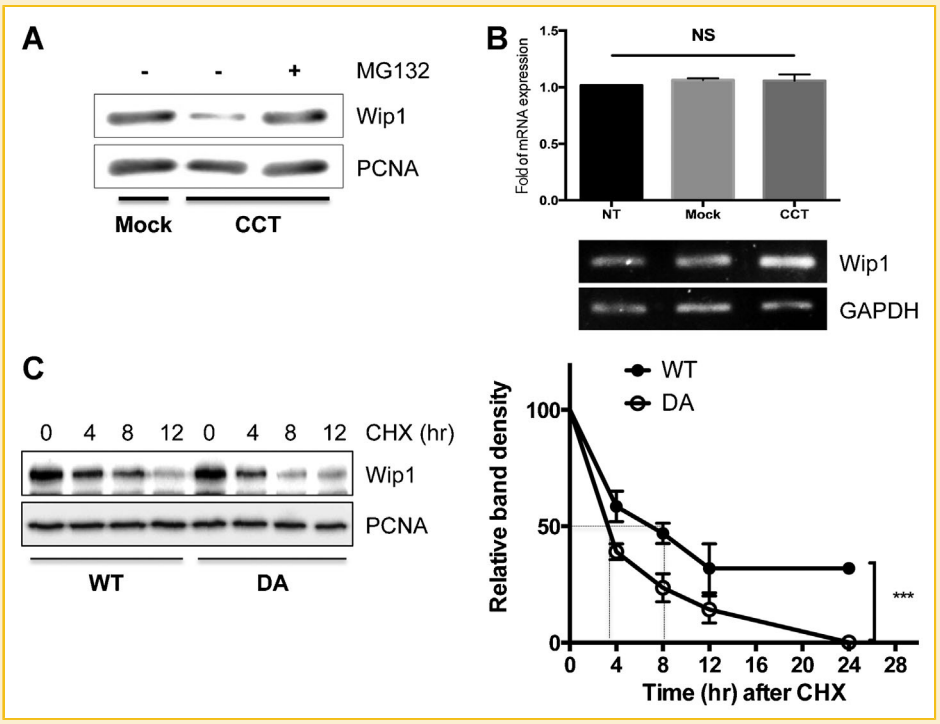

Fig. 4. The phosphatase activity of Wip1 determines its stability. (A) MCF7 cells were treated with 20 μM CCT007093 for 24 h in the absence or presence of 10 μM MG132 for 6 h before harvesting. The Wip1 protein levels were determined by IB analysis. PCNA served as a protein-loading control. (B) The mRNA levels of Wip1 after treatment with DMSO or 20 μM CCT007093 were quantified by real-time PCR (top panel) and RT-PCR analysis (bottom pane). GAPDH served as an equal RNA loading control. (C) Equal levels of Wip1 WT or DA were induced in iWip1-H2B-GFP-HeLa cells, and their protein stabilities after CHX treatment at the indicated times were determined by IB for Wip1. PCNA served as an equal protein-loading control (top panel). The relative band density was measured by a Fusion SOLO chemiluminescence imaging system, and the relative level is presented as a graph (bottom panel).

concomitant expression of Wip1 WT or DA by Dox treatment. As described in Figure 1C and S1C, Wip1 induction was distinct from 8 to 16 h after Dox treatment, which is when cells are ready to exit from mitosis. As shown in Figure 5A, flow cytometric analysis revealed that ectopic expression of WT or DA showed no noticeable change in the cell population at each cell-cycle phase when compared to the control, as previously described by Macurek et al. [2013]. To more closely examine mitotic progression, the pHH3-positive population after G1/S release was determined by flow cytometry. The results revealed that the expression of Wip1 WT, but not DA, during mitosis decreased the peak percentage of the mitotic population (Fig. 5B); these results were contrary to a previous observation [Macurek et al., 2013]. To resolve this discrepancy, the mitotic duration of each individual cell timely expressing WT or DA expression in iWip1-H2B-GFP-HeLa cells was determined by time-lapse microscopy. To our surprise, a significant delay of mitotic progression, especially between metaphase and anaphase, was manifested by mitotic induction of Wip1 WT, but not DA (Fig. 5C). Statistical analysis of the mitotic duration of more than 50 independent cells of each group showed that Wip1 WT-expressing cells significantly retarded mitotic progression compared to the control (Fig. 5D). Detailed assessment of the timing of mitotic sub-phases, such as 'nuclear envelope breakdown (NEB) to metaphase', "metaphase to anaphase" and "anaphase to chromosome decondensation (G1)", indicated that the expression of Wip1 WT, but not DA, significantly delayed the transition from metaphase to anaphase, which was consistent with the results in Figure 5C (Fig. 5E) and when Wip1 was subject to APC/^{Cdh1}-dependent mitotic degradation (Figs. 1–3). In conclusion, mitotic downregulation of Wip1 and/or loss of its phosphatase activity are important pre-requisites for normal mitotic progression.

DISCUSSION

Mitosis is tightly regulated due to sequential phosphorylation and dephosphorylation of mitotic regulatory proteins, which emphasizes the pivotal roles of the timely action of not only kinases but also phosphatases during mitosis [Novak et al., 2010; Hunt, 2013; Seshacharyulu et al., 2013]. In particular, Cdk1 and Cdc25B/C serve a major mitotic kinase and phosphatase, respectively, that predominantly control mitotic phosphorylation and dephosphorylation events. In addition, recent studies revealed that mitotic activation of stress kinases, such as ATM [Yang et al., 2011], CHK1/2 [Kramer et al., 2004; Stolz et al., 2010; Tang et al., 2006] or p38 [Cha et al., 2007], occurs and their activation is engaged in normal mitotic progression. Thereby, perturbation of the timely phosphorylation

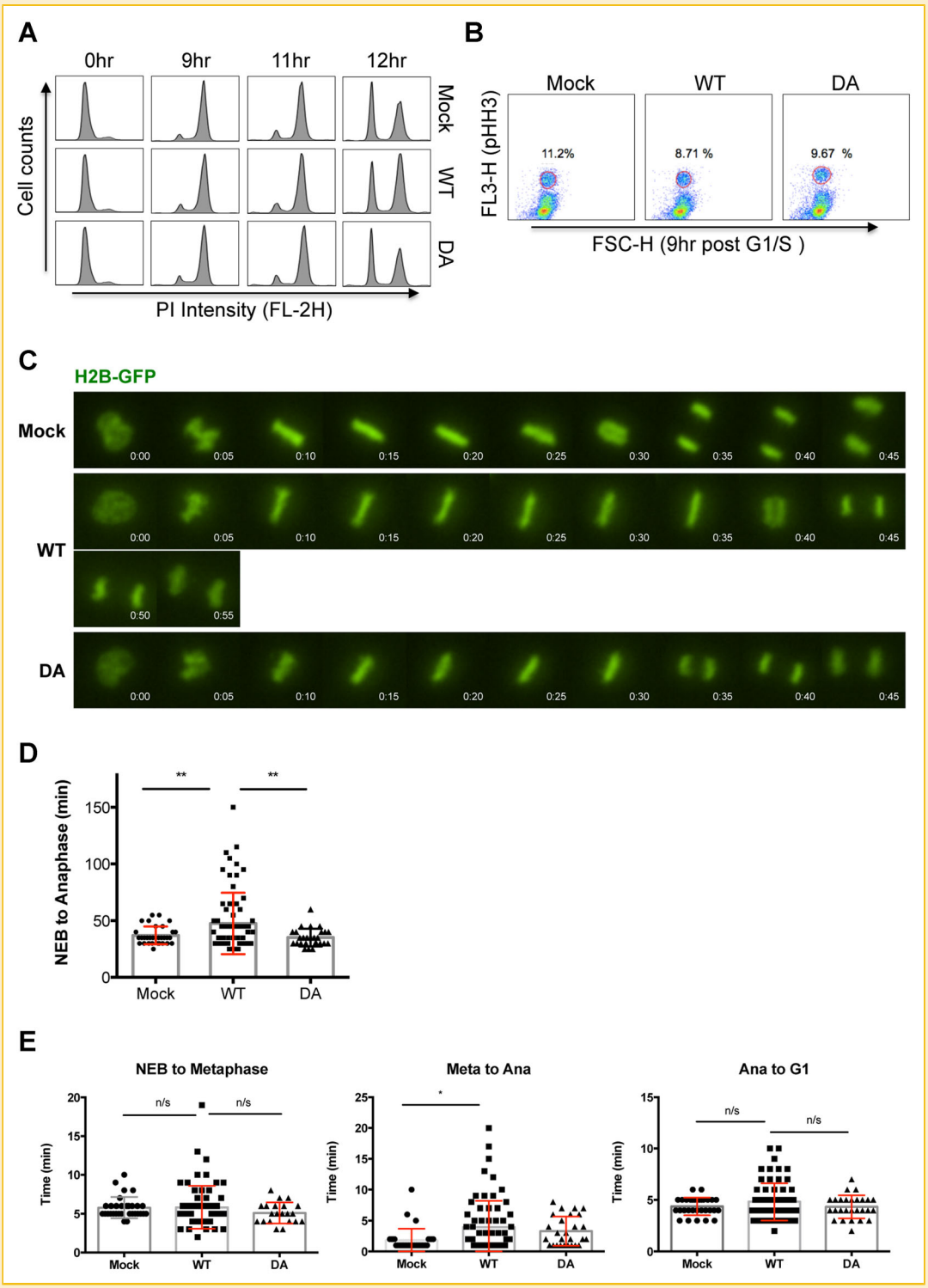

Fig. 5. Wip1 degradation failure delays the anaphase transition. Wip1 WT or DA was induced in iWip1-H2B-GFP-HeLa cells after being released from a DTB. (A) The cell cycle profiles at the indicated times were monitored by flow cytometry with propidium iodide staining. (B) The mitotic index 9 h after release from a DTB was determined by flow cytometry with pH3 (S10). The percentage of the pH3 level is depicted in the graph. (C) Images were captured every 5 min to monitor the mitotic progression of iWip1-H2B-GFP-HeLa cells after WT or DA induction. Still frames from time-lapse movies of representative cells are shown. (D and E) The duration from nuclear envelop breakdown (NEB) to the formation of a metaphase chromosome ("NEB to Metaphase"), from metaphase to anaphase ("Meta to Ana"), and anaphase to G1 ("Ana to G1") were determined at each condition (Mock, WT and DA) ($n >$ "30 to 60"). The duration of each sub-phase is presented as a "scatter plot with bar" graph (n/s: not significant, $^{*} < 0.05$, $^{**} < 0.001$).

status of downstream substrates of such stress kinases leads to either premature mitotic kinase activation [Kramer et al., 2004; Tang et al., 2006], increased chromosome instability [Stolz et al., 2010] or proper onset of mitotic checkpoints [Lee et al., 2010; Yang et al., 2011]. To tightly regulate the phosphorylation status, the proper action of kinases as well as phosphatases should be strictly controlled.

In the present study, we demonstrated that Wip1 phosphatase, whose expression is dependent on a variety of stress stimuli and who serves as a major phosphatase to remove active phosphorylation for homeostasis [Lowe et al., 2012], is downregulated during mitosis (Fig. 1) in a Cdh1-dependent manner (Fig. 3). Most importantly, unlike the previous study [Macurek et al., 2013], disturbance of Wip1 down-regulation by mitotic Wip1 induction clearly delayed the metaphase to anaphase transition (Fig. 5). Of note, the aforementioned stress kinases, including ATM, CHK1/2 and p38, which are novel mitotic regulators, are common substrates of Wip1 phosphatase under the stress condition [Lowe et al., 2012]. Thereby, a sustained phosphorylation status of these stress mediators or their downstream molecules, such as Bub1 [Yang et al., 2011] or Plk1 [Tang et al., 2006], during mitosis by timely deactivation following downregulation of Wip1 may be important for proper mitotic progression. It is noteworthy that among the 700 putative ATM or ATM substrates under the DNA damage condition, a number of proteins in the spindle assembly checkpoint, such as Bub1, Mad1, Sgo1 and Mad2BP, are newly identified as putative substrates of ATM or ATR [Matsuoka et al., 2007]. Considering induction of Wip1 WT, but not DA, during mitosis could significantly weaken ATM-dependent phosphorylation (Fig. S1D), lesser phosphorylation of those molecules during mitosis may be associated with delay of the metaphase to anaphase transition during Wip1 WT induction (Fig. 5C and D). Accordingly, monitoring the alteration of the pS(pT)Q phosphorylation status during mitosis after induction of WT or DA in iWip1-H2B-GFP-HeLa cells would be an interesting approach to identify novel mitotic regulators whose phosphorylation statuses are able to address the mitotic delay during Wip1 induction. Such an interesting possibility remains to be verified in future studies.

In summary, we showed evidence that Wip1 underwent Cdh1-dependent proteolysis during mitosis and sustained Wip1 activity during mitosis, resulting in mitotic delay at the metaphase to anaphase transition. Therefore, we suggest that timely degradation of Wip1 phosphatase by APC/C^{cdh1} is required for normal mitotic progression.

ACKNOWLEDGEMENT

We thank Dr. Surabhi Dangi-Garimella for manuscript review and important comments.

REFERENCES

Belova GI, Demidov ON, Fornace AJ, Jr., Bulavin DV. 2005. Chemical inhibition of Wip1 phosphatase contributes to suppression of tumorigenesis. Cancer Biol Ther 4:1154–1158.

Bulavin D, Amundson S, Fornace, A. Jr. 2002. p38 and Chk1 kinases: Different conductors for the G2/M checkpoint symphony. Curr Opin Genet Dev 12:92–97.

Bulavin DV, Phillips C, Nannenga B, Timofeev O, Donehower LA, Anderson CW, Appella E, Fornace AJ. Jr. 2004. Inactivation of the Wip1 phosphatase inhibits mammary tumorigenesis through p38 MAPK-mediated activation of the p16(Ink4a)-p19(Arf) pathway. Nat Genet 36:343–350.

Cha H, Hancock C, Dangi S, Maiguel D, Carrier F, Shapiro P. 2004. Phosphorylation regulates nucleophosmin targeting to the centrosome during mitosis as detected by cross-reactive phosphorylation-specific MKK1/MKK2 antibodies. Biochem J 378:857–865.

Cha H, Lowe JM, Li H, Lee JS, Belova GI, Bulavin DV, Fornace AJ. Jr. 2010. Wip1 directly dephosphorylates gamma-H2AX and attenuates the DNA damage response. Cancer Res 70:4112–4122.

Cha H, Wang X, Li H, Fornace AJ. Jr. 2007. A functional role for p38 MAPK in modulating mitotic transit in the absence of stress. J Biol Chem 282: 22984–22992.

Cho HJ, Lee EH, Han SH, Chung HJ, Jeong JH, Kwon J, Kim H. 2012. Degradation of human RAP80 is cell cycle regulated by Cdc20 and Cdh1 ubiquitin ligases. Mol Cancer Res 10:615–625.

Ciccia A, Elledge SJ. 2010. The DNA damage response: Making it safe to play with knives. Mol Cell 40:179–204.

Cotto-Rios XM, Jones MJ, Busino L, Pagano M, Huang TT. 2011. APC/CCdh1-dependent proteolysis of USP1 regulates the response to UV-mediated DNA damage. J Cell Biol 194:177–186.

Crescenzi E, Raia Z, Pacifico F, Mellone S, Moscato F, Palumbo G, Leonardi A. 2013. Down-regulation of wild-type p53-induced phosphatase 1 (Wip1) plays a critical role in regulating several p53-dependent functions in premature senescent tumor cells. J Biol Chem 288:16212–16224.

Douarre C, Mergui X, Sidibe A, Gomez D, Alberti P, Mailliet P, Trentesaux C, Riou JF. 2013. DNA damage signaling induced by the G-quadruplex ligand 12459 is modulated by PPM1D/WIP1 phosphatase. Nucleic Acids Res 41: 3588–3599.

Elowe S, Hummer S, Uldschmid A, Li X, Nigg EA. 2007. Tension-sensitive Plk1 phosphorylation on BubR1 regulates the stability of kinetochore microtubule interactions. Genes Dev 21:2205–2219.

Filipponi D, Muller J, Emelyanov A, Bulavin DV. 2013. Wip1 controls global heterochromatin silencing via ATM/BRCA1-dependent DNA methylation. Cancer Cell 24:528–541.

Fiscella M, Zhang H, Fan S, Sakaguchi K, Shen S, Mercer WE, Vande Woude GF, O'Connor PM, Appella E. 1997. Wip1, a novel human protein phosphatase that is induced in response to ionizing radiation in a p53-dependent manner. Proc Natl Acad Sci U S A 94:6048–6053.

Hunt T. 2013. On the regulation of protein phosphatase 2A and its role in controlling entry into and exit from mitosis. Adv Biol Regul 53: 173–178.

Kramer A, Mailand N, Lukas C, Syljuasen RG, Wilkinson CJ, Nigg EA, Bartek J, Lukas J. 2004. Centrosome-associated Chk1 prevents premature activation of cyclin-B-Cdk1 kinase. Nat Cell Biol 6:884–891.

Kurita R, Suda N, Sudo K, Miharada K, Hiroyama T, Miyoshi H, Tani K, Nakamura Y. 2013. Establishment of immortalized human erythroid progenitor cell lines able to produce enucleated red blood cells. PLOS ONE 8:e59890.

Le Guezennec X, Brichkina A, Huang YF, Kostromina E, Han W, Bulavin DV. 2012. Wip1-dependent regulation of autophagy, obesity, and atherosclerosis. Cell Metab 16:68–80.

Lee JS, Park JR, Kwon OS, Kim H, Fornace AJ, Jr. Cha HJ. 2014. Off-target response of a Wip1 chemical inhibitor in skin keratinocytes. J Dermatol Sci 73:125–134.

Lee K, Kenny AE, Rieder CL. 2010. P38 mitogen-activated protein kinase activity is required during mitosis for timely satisfaction of the mitotic checkpoint but not for the fidelity of chromosome segregation. Mol Biol Cell 21:2150–2160.

Liu Z, Yuan F, Ren J, Cao J, Zhou Y, Yang Q, Xue Y. 2012. GPS-ARM: Computational analysis of the APC/C recognition motif by predicting D-boxes and KEN-boxes. PLoS One 7:e34370.

Lowe J, Cha H, Lee MO, Mazur SJ, Appella E, Fornace AJ. Jr. 2012. Regulation of the Wip1 phosphatase and its effects on the stress response. Front Biosci (Landmark Ed) 17:1480–1498.

Macurek L, Benada J, Mullers E, Halim VA, Krejcikova K, Burdova K, Pechackova S, Hodny Z, Lindqvist A, Medema RH, Bartek J. 2013. Downregulation of Wip1 phosphatase modulates the cellular threshold of DNA damage signaling in mitosis. Cell Cycle 12:251–262.

Manchado E, Eguren M, Malumbres M. 2010. The anaphase-promoting complex/cyclosome (APC/C): Cell-cycle-dependent and -independent functions. Biochem Soc Trans 38:65–71.

Matsuoka S, Ballif BA, Smogorzewska A, McDonald ER, 3rd, Hurov KE, Luo J, Bakalarski CE, Zhao Z, Solimini N, Lerenthal Y, Shiloh Y, Gygi SP, Elledge SJ. 2007. ATM and ATR substrate analysis reveals extensive protein networks responsive to DNA damage. Science 316:1160–1166.

Nakayama KI, Nakayama K. 2006. Ubiquitin ligases: Cell-cycle control and cancer. Nat Rev Cancer 6:369–381.

Novak B, Kapuy O, Domingo-Sananes MR, Tyson JJ. 2010. Regulated protein kinases and phosphatases in cell cycle decisions. Curr Opin Cell Biol 22: 801–808.

Oricchio E, Saladino C, Iacovelli S, Soddu S, Cundari E. 2006. ATM is activated by default in mitosis, localizes at centrosomes and monitors mitotic spindle integrity. Cell Cycle 5:88–92.

Peters JM. 1998. SCF and APC: The Yin and Yang of cell cycle regulated proteolysis. Curr Opin Cell Biol 10:759–768.

Peters JM. 2002. The anaphase-promoting complex: Proteolysis in mitosis and beyond. Mol Cell 9:931–943.

Peters JM. 2006. The anaphase promoting complex/cyclosome: A machine designed to destroy. Nat Rev Mol Cell Biol 7:644–656.

Raff JW, Jeffers K, Huang JY. 2002. The roles of Fzy/Cdc20 and Fzr/Cdh1 in regulating the destruction of cyclin B in space and time. J Cell Biol 157: 1139–1149.

Rayter S, Elliott R, Travers J, Rowlands MG, Richardson TB, Boxall K, Jones K, Linardopoulos S, Workman P, Aherne W, Lord CJ, Ashworth A. 2008. A chemical inhibitor of PPM1D that selectively kills cells overexpressing PPM1D. Oncogene 27:1036–1044.

Seshacharyulu P, Pandey P, Datta K, Batra SK. 2013. Phosphatase: PP2A structural importance, regulation and its aberrant expression in cancer. Cancer Lett 335:9–18.

Shaltiel IA, Aprelia M, Saurin AT, Chowdhury D, Kops GJ, Voest EE, Medema RH. 2014. Distinct phosphatases antagonize the p53 response in different phases of the cell cycle. Proc Natl Acad Sci USA 111:7313–7318.

Shen K, Wang Y, Brooks SC, Raz A, Wang YA. 2006. ATM is activated by mitotic stress and suppresses centrosome amplification in primary but not in tumor cells. J Cell Biochem 99:1267–1274.

Stolz A, Ertych N, Kienitz A, Vogel C, Schneider V, Fritz B, Jacob R, Dittmar G, Weichert W, Petersen I, Bastians H. 2010. The CHK2-BRCA1 tumour suppressor pathway ensures chromosomal stability in human somatic cells. Nat Cell Biol 12:492–499.

Sun B, Hu X, Liu G, Ma B, Xu Y, Yang T, Shi J, Yang F, Li H, Zhang L, Zhao Y. 2014. Phosphatase Wip1 negatively regulates neutrophil migration and inflammation. J Immunol 192:1184–1195.

Tang J, Erikson RL, Liu X. 2006. Checkpoint kinase 1 (Chk1) is required for mitotic progression through negative regulation of polo-like kinase 1 (Plk1). Proc Natl Acad Sci U S A 103:11964–11969.

Teixeira LK, Reed SI. 2013. Ubiquitin ligases and cell cycle control. Annu Rev Biochem 82:387–414.

Xia Y, Ongusaha P, Lee SW, Liou YC. 2009. Loss of Wip1 sensitizes cells to stress- and DNA damage-induced apoptosis. J Biol Chem 284:17428–17437.

Yamaguchi H, Durell SR, Chatterjee DK, Anderson CW, Appella E. 2007. The Wip1 phosphatase PPM1D dephosphorylates SQ/TQ motifs in checkpoint substrates phosphorylated by PI3K-like kinases. Biochemistry 46:12594–12603.

Yang C, Tang X, Guo X, Niikura Y, Kitagawa K, Cui K, Wong ST, Fu L, Xu B. 2011. Aurora-B mediated ATM serine 1403 phosphorylation is required for mitotic ATM activation and the spindle checkpoint. Mol Cell 44:597–608.

Zhang H, Shi X, Paddon H, Hampong M, Dai W, Pelech S. 2004. B23/nucleophosmin serine 4 phosphorylation mediates mitotic functions of polo-like kinase 1. J Biol Chem 279:35726–35734.

Zhang X, Wan G, Mlotshwa S, Vance V, Berger FG, Chen H, Lu X. 2010. Oncogenic Wip1 phosphatase is inhibited by miR-16 in the DNA damage signaling pathway. Cancer Res 70:7176–7186.

SUPPORTING INFORMATION

Additional supporting information may be found in the online version of this article at the publisher's web-site.